ELSEVIER

Quantum dot field effect transistors

Frederik Hetsch[1], Ni Zhao[2], Stephen V. Kershaw[1] and Andrey L. Rogach[1,*]

[1] Department of Physics and Materials Science and Centre for Functional Photonics (CFP), City University of Hong Kong, Hong Kong Special Administrative Region
[2] Department of Electronic Engineering, The Chinese University of Hong Kong, Hong Kong Special Administrative Region

Solution processed colloidal semiconductor quantum dots offer a high potential for decreasing costs and expanding versatility of many electronic and optoelectronic devices. Initially used as a research tool to study charge carrier mobilities in closely packed quantum dot thin films, field effect transistors with quantum dots as the active layer have recently experienced a breakthrough in performance (achievement of mobilities higher than 30 $cm^2 V^{-1} s^{-1}$) as a result of a proper choice of surface ligands and/or improved chemical treatment of the nanoparticle films during device processing. Here we review these innovative developments and the continuing work that may soon lead to commercial grade electronic components.

Introduction

The use of colloidal quantum dots (QDs) in films for electronic and optoelectronic applications was suggested soon after the discovery of a quantum size effect in these semiconductor nanostructures [1,2]. Since then the advantages of inexpensive solution processed colloidal QDs such as size tunable band gap, a small exciton binding energy and high photoluminescence (PL) quantum yields have been successfully demonstrated in thin film optoelectronic devices, for example, in solar cells and light-emitting diodes [3,4]. Yet, charge transport measurements on QD films in field-effect transistors (FETs) have shown rather limited promise, lagging well behind commercial silicon and even organic active channel FETs until recently, largely as a result of poor carrier mobilities due to the choice of interparticle ligand materials. In the following sections we describe the synthesis of colloidal QDs with traditional long chain organic ligands, the device physics of QD based FETs, and go on to discuss the development of chemical treatments that are now being applied to vastly improve QD active channel FET performance.

Quantum dot synthesis

Colloidal semiconductor QDs can be synthesized by a wide variety of wet chemistry techniques in both aqueous and organic solvents, and even in mixed solvents at the interface between water and organic phases or within microemulsions or aerosols [5]. There are several generic ligand based approaches to stabilize the growing inorganic nanoparticles. For some II-VI or III-V semiconductor QDs there is a clearly preferred type of synthesis to grow good quality particles, for example, on the basis of growth temperature and growth kinetics to favour particles with a high degree of crystallinity, a particular mean size and size distribution [6,7], and particle shape. In the latter respect, particles with near spherical shape are generally desirable for regular, close (hexagonally) packed films. Equally, regularly shaped (i.e. monodisperse) cube shaped nanocrystals can be grown and have been shown to pack into regular arrays with good quality, and can have superior transport properties [8,9] to spherical particle arrays due to the lower average interparticle spacing. For the III-Vs and several II-VI and IVB-IV QDs, growth using the hot injection method derived from the early work of Murray *et al.* [7,10], when optimized, is generally found to produce good quality particles with well defined size, shape [11], and material quality. The basic hot injection synthesis method is outlined in Fig. 1. In most cases the metal precursor in the main reaction flask is initially held at a given temperature and the anion precursor, for example, TOP-Se (trioctylphosphine selenide), or $(TMS)_2$-Se (bis(trimethylsilyl) selenide) is injected. Often the growth temperature is lower than the nucleation temperature (sometimes the lowering may be achieved conveniently by the injection of the cooler precursor alone). In some cases the reverse arrangement may be used, where the metal

*Corresponding author:. Rogach, A.L. (andrey.rogach@cityu.edu.hk)

 1369-7021/06/$ - see front matter http://dx.doi.org/10.1016/j.mattod.2013.08.011

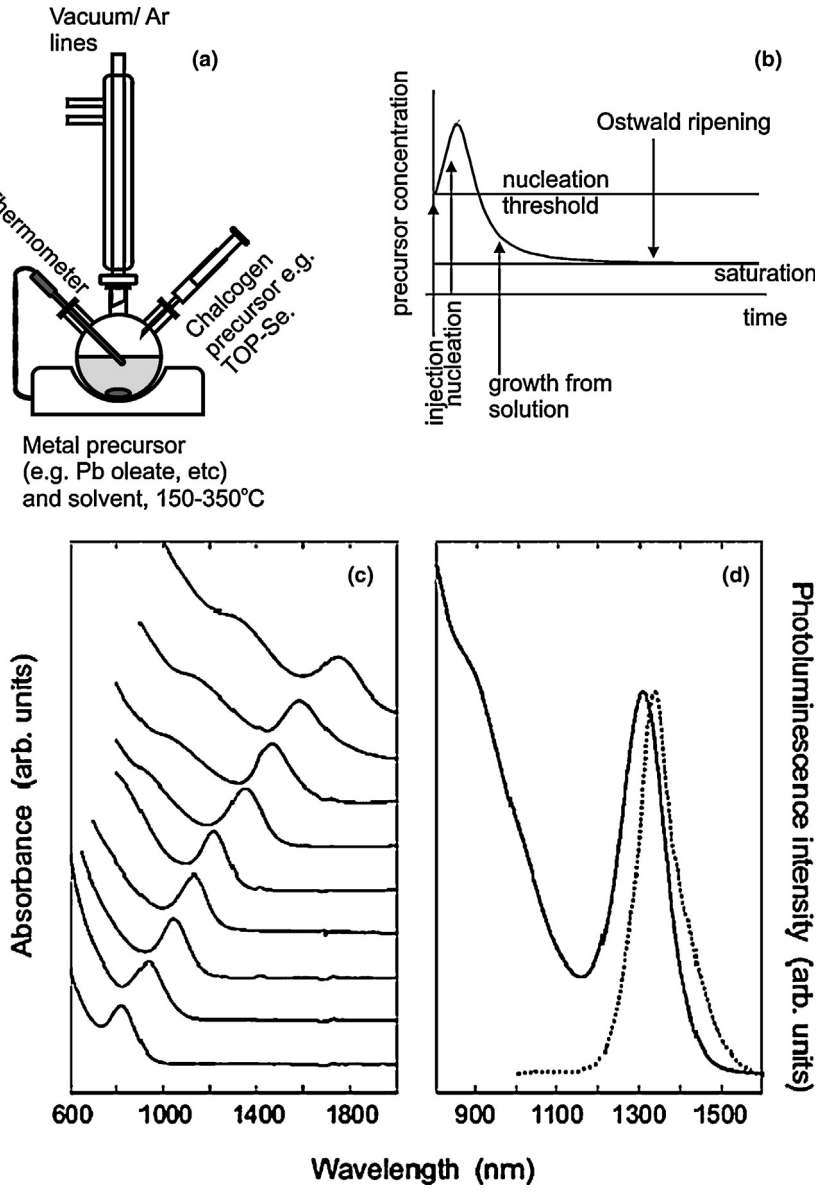

FIGURE 1

(a) Hot injection synthesis method. (b) Trajectory for the precursor concentration, assuming a single initial injection of the latter. (c) Typical evolution of the band edge absorption of PbS QDs with growth duration. (d) PL and absorption for 6.5 nm PbS particles. (c and d) Reproduced from Hines and Scholes [12]. Copyright 2003, WILEY-VCH Verlag GmbH & Co. KGaA, Weinheim; with permission from John Wiley & Sons, Inc.

precursor is injected into a hot chalcogenide (or pnictide in the case of III-V QDs, among others) precursor solution. Figure 1b shows the transitions from nucleation, through growth from solution, followed by Ostwald ripening and finally to saturation.

Apart from PbSe (as exemplified in Fig. 1a), the hot injection method has been used to grow good quality QD materials including PbS [12–15], and most notably with relevance to early FET work, CdSe [7,16]. In early work on III-V QDs growth temperatures were quite high (e.g. 265 °C for InAs [17]) and the resulting QD size distribution could be quite broad. More recently InSb QDs have been grown using a modified synthesis [18] with lithium bis(trimethylsilyl)amide ($Li[N(Si(Me)_3)_2]$ used to improve the nucleation process, resulting in material with a 15% size distribution which could readily be narrowed by a size selective precipitation process.

For some materials, especially where higher (e.g. >100 °C) growth temperatures are not suitable [19], there may be less of a clear cut case in favour of the hot injection route – this is more the case for materials such as HgTe, CdTe [20,21] or $Cd_xHg_{1-x}Te$ alloy QDs [22] where room temperature or low temperature (<100 °C) aqueous methods may lead to equally useful material and for FET devices may also offer the benefit of the use of short chain, charge stabilizing rather than long chain sterically stabilizing organic ligands.

For FET devices the basic requirement is that good quality thin films (one to several or even a few tens of QD diameters in thickness), can be formed from the QD precursor solution. This requirement is readily met by QDs grown by the hot injection method: QDs with near monodisperse size distribution can be grown or directly transferred (after washing) into volatile solvents (e.g. hexane, toluene, acetone, among others) suitable for spin coating/layer by layer QD deposition methods. The use of long chain aliphatic ligands (such-like mercapto alkyls, alkyl

phosphonic compounds, metal oleates) however is a distinct disadvantage for high carrier mobility films as such materials are effective dielectric insulators. In contrast aqueous QDs may be grown with relatively short chains (e.g. thioglycerol, mercaptopropionic acid, among others) but deposition of good quality films from aqueous solution is problematic due to the low solvent volatility. The much higher zeta potential (measure of surface charge) in aqueous QDs may also hinder the formation of close packed films due to the presence of strong interparticle repulsions if steps are not taken to reduce this. The latter could be achieved by changing the solution pH or adding small ions to screen the charge just prior to deposition.

Good quality thin films are obtained if the QDs are regularly and densely (i.e. close) packed. For simple single component QDs this is favoured where the QD size distribution is narrow and QDs are near spherical in shape [23]. The deposition process and the usual ligand exchange stage for FET structures mean that extended range close packing is unlikely, but close packed domains of perhaps 10–100 nm can be formed. On the larger length scale (>100 nm) the packing is somewhat more randomly arranged, that is, ordering is restricted to finite domains. However recent advances in techniques for the growth of QD and other nanoparticle superlattices [24,25] (also termed colloidal crystals) which can maintain the ordered packing on up to 0.1 mm length scales offers some hope that deposition techniques may *in the future* be developed to allow such regularly packed QD structures (with appropriately short ligands) to be fabricated in thin film form suitable for FET structures.

Fabrication of QD FETs

For the fabrication of a quantum dot FET, two configurations are widely used (Fig. 2). For the bottom-gate configuration, a highly doped silicon wafer is used as a gate separated from the QD film with a dielectric (e.g. SiO_2). On this substrate two electrodes, source and drain, are either pre-patterned by optical lithography and evaporation of a metal or post-patterned via shadow mask evaporation. The QD film is deposited by different methods, for example, by drop casting or spin coating. For the top-gate configuration, after the deposition of electrodes and QD films a dielectric layer (e.g. SiO_2, Al_2O_3, or an ion gel) is formed on top. This dielectric layer separates the top gate from the QD film. For measurements, voltage is applied to the gate and the drain while the source is grounded [3].

Silicon substrate based FETs are most commonly used for material characterization but there are also reports of polymer substrate FETs [26] for both characterization and most importantly to demonstrate the great potential of QDs to form FET electronic circuitry on low cost, flexible materials and moreover using low process temperatures to fabricate them.

Principle of FET operation

When a voltage is applied between the source and gate of a QD FET, charges are injected from the source and accumulate at the semiconductor-insulator interface. If the voltage exceeds a threshold, V_T, a conducting channel is established. The application of a bias across the source and drain will then result in a drain-to-source current (I_{DS}). At low drain voltages, I_{DS} increases linearly with the drain voltage. Therefore the transistor is said to operate

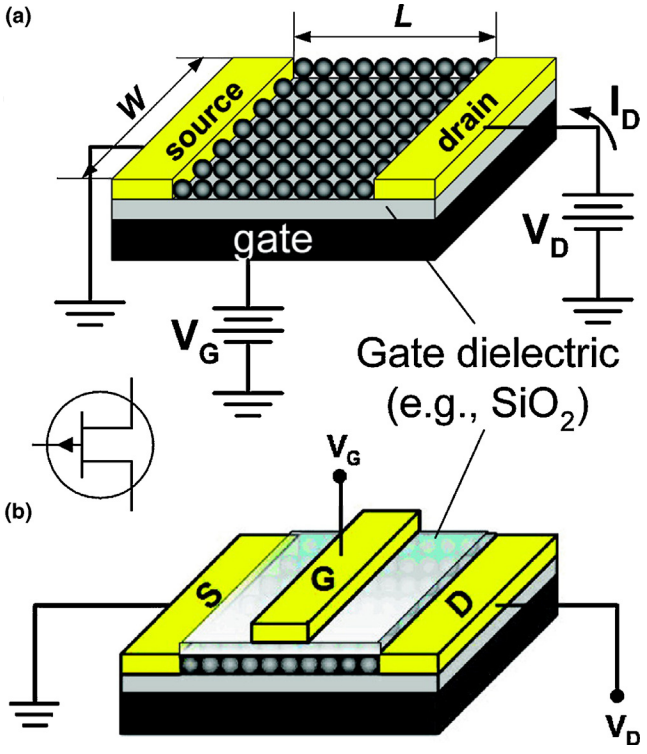

FIGURE 2

Basic configurations of QD based field-effect transistors (FET): (a) bottom-gate FET; (b) top-gate FET. *L* and *W* show transistor channel length and width, respectively. S, D, and G are the source, drain, and gate electrodes (terminals). Reprinted with permission from Ref. [3]. Copyright 2010 American Chemical Society.

in the *linear regime* and the current–voltage equation can be simplified as (Eqn 1) [27]:

$$I = \left(\frac{W}{L}\right)\mu_{lin}C_i(V_G - V_T)V_D \quad (1)$$

where W and L are the channel width and length, respectively, μ_{lin} is the field-effect mobility in the linear regime, C_i is the capacitance density (per unit area) of the gate insulator, and V_G and V_D are the gate and drain voltages, respectively. When V_D exceeds $(V_G - V_T)$, the free charge density in the vicinity of the drain contact decreases to approximately (but not quite) zero. This is called channel *pinch off*. At this condition, a further increase in the drain voltage will not enhance the drain current, and the device is said to operate in the *saturation regime*. The current is then given by (Eqn 2) [3]:

$$I = \left(\frac{W}{2L}\right)\mu_{sat}C_i(V_G - V_T)^2 \quad (2)$$

where μ_{sat} is the mobility in the saturated regime.

In both (Eqn 1) and (Eqn 2) a knowledge of C_i is required to extract the mobilities and this is simply calculated as (Eqn 3):

$$C_i = \frac{WL\varepsilon\varepsilon_0}{d} \quad (3)$$

where values for the gate dielectric thickness, d, and the (static) permittivity of the dielectric material, ε, are required. A range of gate dielectrics have been used in conjunction with QD FETs and their use often stems from earlier work on organic FETs and indeed also from the search for high permittivity dielectrics for the

TABLE 1

Values of gate dielectric relative permittivities.

Dielectric	ε_r		Ref.
SiO_2	3.9	Thin films → high leakage currents (tunnelling)	[28,31]
Al_2O_3 (not ALD)	9.0	High K dielectric	[26,28]
Ion gel	[a]	For example, 10 wt% triblock–copolymer and 90 wt% ionic liquid	[29,30,32]
SAM (ODPA) Octadecyl phosphonic acid	2.5	Tunnelling barrier/hydrophobic group to lower gate leakage current and hysteresis in composite dielectrics	[33]
SAM (OTS) Octadecyl trichlorosilane	2.5	Tunnelling barrier/hydrophobic group to lower gate leakage current and hysteresis in composite dielectrics	[31]
PMMA	2.6		[34]
CYTOP	~2	Hydrophobic, highly fluorinated polymer. Low hysteresis and tunnelling current	[35]
ZrO_x (from sol gel)	~9	Stoichiometry dependent	[35]
Polyimide	3.05	PI-2611, from HD MicroSystems	[36]
Parylene-C	3.15		[36]
Si_3N_4	7.5		[36]
Si_3N_4	7	High K dielectric	[28]
Ta_2O_5	22	High K	[28]
TiO_2	80	High K	[28]
$SrTiO_3$	2000	Para-electric high K	[28]
ZrO_2	25	High K	[28]
HfO_2	25	High K	[28]
$HfSiO_4$	11	High K	[28]
La_2O_3	30	High K	[28]
Y_2O_3	15	High K	[28]
a-$LaAlO_3$	30	High K	[28]

[a] For ion gels the precise gate geometry is often not well defined. Cho *et al.* [30] estimate that specific gate capacitances comparable to HfO_2 and Ta_2O_5 (better than 1 μF/cm^2) can be achieved with typical ion gels.

mainstream CMOS industry when gate dielectric thicknesses are being pushed to their limits [28]. Table 1 lists a number of such gate dielectrics with their relative permittivity values. While some of the refractory materials have very high permittivity values, as Robertson [28] discusses, there may yet be problems with film crystallinity which limit their application. Ion gels can be useful to generate very high polarization [29,30] but fabrication of FETs with such materials in the gate structure has tended to be less compatible with mass manufacturing methods to date. For now, it seems that the best rational compromise in terms of potentially commercializable structures would be an Al_2O_3 gate dielectric, which can be topped with a surface monolayer of alkylphoshonic acid or alkylchlorosilane if leakage current and moisture sensitivity are major concerns. However, new gate dielectric materials are being continually developed and this may yet be superseded.

The principal QD FET figures-of-merit include the field-effect mobility, the current on-to-off ratio, the threshold voltage and the sub-threshold slope. In crystalline inorganic semiconductors, charges transport in a delocalized manner (band-like transport), and the main limiting factor for the field-effect mobility is the scattering of charges by phonons or impurities. In QD films the inter-dot coupling with long chain synthesis ligands is relatively weak, and although shorter ligands improve this (as discussed in later sections) coupling is still insufficient to show true demonstrable band-like transport as seen in silicon. This results in the charge carriers being highly localized and moving by tunnelling or thermally assisted hopping between QDs. Therefore the field-effect mobility of QD films can be influenced by the inter-dot distance, temperature and distribution of trap states. V_T corresponds to the point at which the majority of the deep traps are filled and meaningful transport occurs. The threshold voltage is therefore a measure of the initial concentration of charge carriers [37] or in other words for the Fermi level in the film [38] (see Fig. 6b). A lower V_T reflects a higher doping level of the QD film [37]. The sub-threshold slope (SS) can be derived from Eqn 4 [3],

$$SS = \frac{dV_G}{d(\log I_d)} \quad (4)$$

Steep SS is highly desired since it improves the ratio between the on- and off-currents at the turn-on voltage and makes the FET more energy efficient.

The development of QD FET materials and films

The development of QD FETs has its roots in the early work on photoconductivity and related electrochemical studies. The groups of Vanmaekelbergh [39–44], and Guyot-Sionnest [7,45,46], made major contributions to the understanding of charge transport in QD films. These studies were essentially on QD electrochemical transistors, in which a reference electrode in an electrochemical cell is used instead of a gate electrode, and helped lay the foundations for the later solid film QD FETs by developing the models for the basis of charge transport in QD films.

Measurements on FETs with different QD materials have shown that the electrical conductivity in as-synthesized, untreated QD films is extremely low [47]. The low conductivity is attributed to long-chain dielectrically isolating ligand molecules that are used in the synthesis and a high number of surface dangling bonds due to unpassivated surface atoms which hinder charge transport by trapping charge carriers in mid-gap states [47–50]. Materials that were shown to be insulating include HgTe [51], SnTe [52], PbTe [53,54], PbSe [32,55,56], PbS [56] and CdSe [57–59]. These measurements showed that the films of colloidal semiconductor QDs

have to be post-preparatively treated for their successful application in electronic or optoelectronic devices. This was in fact also realized very early in the development of QD film devices, preceding even the first demonstrations of QD FETs. In their work on electrochromism in CdSe films [60], the Guyot-Sionnest group were the first to show the benefits of ligand exchange with short chain bifunctional molecules to reduce interparticle spacings and so improve the carrier mobilities and thereby electro-optic response times in their devices. In early studies on the photoconductivity of CdSe films Leatherdale *et al.* [61] had already made the correlation between the QD interparticle spacing and photoionization efficiencies, a useful measure of the barrier to charge transport posed by the presence of a number of different organic passivating ligands and core–shell structures in their case. In 2004 the Bawendi group then applied the same bifunctional amine ligand replacement approach suggested by Guyot-Sionnest's group and using a range of different length diamine molecules (giving a range of particle spacings from 1.1 nm down to 0.06 nm (with sodium hydroxide treatment) were able to show vastly improved photoionization efficiencies (approaching unity) with the reduced dielectric spacing between particles [62].

The synergy between FET and photoconductivity research still continues. The more recently developed time-resolved microwave conductivity (TMRC) measurement method has been applied to CdSe and PbSe QD films by Talgorn and co-workers [63–65] to probe not only mobilities but also photoionization efficiencies and to follow the temporal behaviour of photoinduced carriers. The TMRC method has distinctly appealing benefits – small domains can be probed (~few 10s nm scale) reducing the influence of physical cracks in the film on the measurement. In addition, it is an electrode-free technique, eliminating the influence of carrier injection issues at the contact with the QD film. Thus TMRC can probe the intrinsic carrier dynamics. Again, with ligand exchange the technique has been used to probe the influence of the exchange ligand head groups and carrier length on the intrinsic transport properties [65].

In the development of QD FETs, several more groups have shown different types of treatments to improve mobilities that can be classified into two categories based upon the effect on the conductivity. One way to increase the conductivity of the films is to improve the charge carrier transport. In this case, treatments are used to reduce the interparticle distance between the QDs [47,66]. The first experiments used annealing and sintering as a way to contract the interparticle separation [1]. Very soon several groups started to exchange ligands on the QDs from long alkyl chain ligands like oleaic acid that were used in the synthesis to shorter organic molecules such as thiols or amines [67,68]. A ligand exchange can be done either post-synthesis in solution [57] or post-deposition in film [55]. Several groups showed ligand exchange substituting inorganic complexes, foremost Talapin *et al.* using inorganic metal chalcogenide complexes (MCCs) [69]. The second way to improve conductivity in QD films is by chemical doping. Although, chemical doping in QDs brings new challenges when compared to the doping of bulk semiconductors [70] this approach, as exemplified by Choi and co-workers' doping of CdSe QDs with In, led to impressive mobilities and reports of band-like transport [71].

The comparative benefits of each improvement method can be gauged with the aid of Table 2. In this table we summarize each of the different treatments, organized by sections, and their effects on the conductivity in different QD materials. Clearly, CdSe and PbSe are the workhorses for QD FET research. However, the successful application of a chemical treatment in one material might guide the way for improvements in others. Also, the table clearly shows that starting from extremely low conductivities in the early works, in 2012 mobilities higher than 30 $cm^2 V^{-1} s^{-1}$ have been achieved in QD FETs. In the following sections we will describe each of the different methods to improve the conductivity in different QD film materials in more detail and we will argue that the breaking of the 30 $cm^2 V^{-1} s^{-1}$ limit in 2012 opened up a whole new perspective towards commercial grade electronic components.

While this Review focuses on the development of QD FETs it is also of interest at this point to compare recent progress on (single) nanowire FETs. Here of course the scale of the nanowires is such that individual wires may be mounted in an FET structure (or rather the FET source and drain electrodes fabricated around an individual isolated wire). Kagan *et al.* [83] have recently shown an impressive hole mobility of 1000 $cm^2 V^{-1} s^{-1}$ in *p*-type PbSe single nanowires at cryogenic temperatures. At the same low temperatures, electron mobilities reached around 150 $cm^2 V^{-1} s^{-1}$. Remote doping with oxygen (in the ppm) range was used.

Methodologies for improvement of charge transport

Annealing/sintering

Annealing and sintering of quantum dot films to increase the conductivity, has been shown in a range of QD materials. The optimal annealing time and temperature can be determined for different ligand molecules by thermogravimetric analysis [84]. In 2002 the annealing process in CdSe solid films was shown to have three major effects [85]: transmission electron micrographs showed that the distance between the particles in the film was reduced; the excitonic peaks of the QDs were red-shifted and broadened; finally, the decreased interparticle space and chemical transformations in the organic ligand molecules led to an increased tunnelling rate and consequently to an increase in the current [85]. Drndič *et al.* showed improvements in FET performance of annealed PbSe QD films [84,86]. By annealing the nominally 1 nm thick insulating oleic acid shell around the QDs, the current increased from negligible, that is, less than 10fA, to several pA [84]. At the same time, the authors showed that with reduced interparticle spacing the transport changed from insulating, dominated by Coulomb blockade to semiconducting [84]. In the latter regime transport was dominated by nearest neighbour hopping of the carriers (NNH) [84]. Further electronic transport measurements from Bawendi *et al.* on annealed PbSe QD solids could also be described by hopping between intrinsic localized states [87]. Kim *et al.* sintered HgTe QD films and reported hole mobilities reaching 0.82 $cm^2 V^{-1} s^{-1}$ in a bottom-gate configuration and 2.38 $cm^2 V^{-1} s^{-1}$ in a top-gate configuration, with SiO_2 and Al_2O_3 as the respective dielectric layers [74].

These earlier examples showed that as-synthesized QD films can become more conductive upon heat treatment. However, in most cases the temperatures needed to remove long-chain organic ligands by heat alone are high enough to sinter the remaining QDs which thereby eliminates quantum confinement [57]. Furthermore, sintering often transforms the QD solid into a polycrystalline film with structural defects [47]. Consequently, the achieved mobilities remained rather limited.

TABLE 2

Overview of different treatments and the effect on mobilities in quantum dot FETs.

QD material	Treatment	Mobilities [$cm^2 V^{-1} s^{-1}$]	FET configuration	Ref.	Year
Carbon	Ligand exchange with pyridine	8.49×10^{-5} (electron)/3.88×10^{-5} (hole)	Bottom-gate	[68]	2013
CdSe	Ligand exchange with MCCs ($Sn_2S_6^{4-}$) in solution	3×10^{-2} (electron)	Bottom-gate	[69]	2009
CdSe	Inorganic ligand-exchange with NaOH	0.6 (electron)	Top-gate	[72]	2010
CdSe	Inorganic ligand-exchange with MCC $In_2Se_4^{2-}$	16 (electron)	Bottom-gate	[59]	2011
CdSe	Inorganic ligand-exchange with NH_4SCN	3 (electron)	Bottom-gate	[73]	2011
CdSe	Inorganic ligand-exchange with MCC $In_2Se_4^{2-}$ and RTA	38 (electron)	Bottom-gate	[35]	2012
CdSe	Inorganic ligand-exchange with NH_4SCN and doping with In	27 (electron)	Bottom-gate	[71]	2012
CdSe	Inorganic ligand-exchange with S^{2-} and annealing	1.9 (electron)	Bottom-gate	[35]	2012
HgTe	Sintered	0.82 (hole)/2.38 (hole)	Bottom-gate/ Top-gate	[74]	2006
InAs	Ligand exchange in solution (TOP to aniline) and EDA treatment in film	1.2×10^{-5} (lin) (electron)	Bottom gate	[75]	2010
InAs	Ligand exchange with MCCs ($Cu_7S_4^-$) in solution with RTA	16.0 (lin), 14.8 (sat) (electron)	Bottom-gate	[76]	2013
InAs	Ligand exchange with MCCs ($Cu_7S_4^-$) in solution with RTA	3.48 (electron)	Bottom-gate	[76]	2013
InAs	Ligand exchange with MCCs ($Sn_2S_6^{4-}$) in solution with RTA	3.96 (lin), 1.77 (sat) (electron)	Bottom-gate	[76]	2013
InAs	Ligand exchange with MCCs ($Sn_2S_6^{4-}$) in solution with RTA	0.61 (lin), 0.27(sat) (electron)	Bottom-gate	[76]	2013
InAs	Ligand exchange with MCCs ($Sn_2Se_6^{4-}$) in solution with RTA	1.9 (lin), 0.9 (sat) (electron)	Bottom-gate	[76]	2013
InAs	Ligand exchange with MCCs ($Sn_2Se_6^{4-}$) in solution with RTA	0.33 (lin), 0.39 (sat) (electron)	Bottom-gate	[76]	2013
InAs	Ligand exchange with MCCs ($In_2Se_4^{2-}$) in solution with RTA	3.35 (lin), 0.72 (sat) (electron)	Bottom-gate	[76]	2013
InAs	Ligand exchange with MCCs (S^{2-}) in solution with RTA	0.85 (lin), 0.6 (sat) (electron)	Bottom-gate	[76]	2013
InP	Ligand exchange with MCCs ($Sn_2S_6^{4-}$) in solution with RTA	0.09 (lin), 0.05 (sat) (electron)	Bottom-gate	[76]	2013
InP	Ligand exchange with MCCs ($Sn_2Se_6^{4-}$) in solution with RTA	0.07 (lin), 0.04 (sat) (electron)	Bottom-gate	[76]	2013
InP	Ligand exchange with MCCs ($In_2Se_4^{2-}$) in solution with RTA	2×10^{-4} (lin), 1.2×10^{-3} (sat) (electron)	Bottom-gate	[76]	2013
InSb	Ligand exchange with S^{2-} in solution	1.5×10^{-4} (electron), 6×10^{-4} (hole)	Bottom-gate	[18]	2012
PbS	Ligand exchange in solution with butylamine, EDT treated in film	1×10^{-4} (hole)	Bottom-gate	[67]	2008
PbS (cubes)	Ligand exchange with SCN in film	0.04 (hole and electron)	Bottom gate (parylene dielectric)	[9]	2011
PbS (spheres)	Ligand exchange with SCN in film	0.02 (hole and electron)	Bottom gate (parylene dielectric)	[9]	2011
PbS	Atomic-ligand passivation with halide anions	Up to 4×10^{-2} (electron)	Bottom-gate	[77]	2012
PbSe	Ligand exchange with hydrazine	0.9 (electron)/0.2 (hole)	Bottom-gate	[47]	2005
PbSe	Ligand exchange with hydrazine	1.2 (electron)	Bottom-gate	[78]	2008
PbSe	Ligand exchange with EDT	0.07 (electron)/0.03 (hole)	Bottom-gate	[79]	2010
PbSe	Ligand exchange with formic acid	0.3 (hole)	Bottom-gate	[56]	2010
PbSe	Ligand exchange with EDT, atomic layer deposition of Al_2O_3 and ZnO	1.05 (electron)/0.04 (hole)	Bottom-gate	[80]	2011
PbSe	Ligand exchange with SCN in film and additional Pb deposition	9 (lin), 11 (sat) (electron)	Bottom gate	[81]	2013
PbSe	Ligand exchange with SCN in film and additional Se deposition	0.3 (lin), 0.5 (sat) (hole)	Bottom gate	[81]	2013
PbSe	Ligand exchange with S^{2-} in film and additional alumina ALD	9.6 (electron), 0.6 (hole)	Bottom gate	[82]	2013

Ligand exchange

As mentioned already, from the very earliest work by Talapin and Murray [47] mobility improvements in PbSe films were obtained with an amine based exchange ligand, it soon became obvious that further efforts to improve charge transport needed to concentrate on the surface of QDs. Ligand exchange (by chemical means) seemed to be a feasible way to replace bulky organic ligands with shorter ligands [88] to improve charge transport. There have been many studies based on this approach and these are discussed below, grouped by the chemical functionality of the substituting ligands (rather than chronologically).

Thiols

Several groups showed ligand exchange on (hot injection grown) PbSe films with ethanedithiol (EDT) [55,89,90]. Figure 3a shows that after EDT ligand exchange the interparticle spacing in the PbSe film decreased by about 16 Å. However, the quantum dot film also became disordered (Fig. 3a) and cracked widely (Fig. 3c) [55]. Law *et al.* extended the thiol treatment research with a systematic series of alkane-dithiol ligand-exchanged PbSe films [79]. This way the carrier mobility could be correlated with the ligand lengths. A treatment with 1,2-ethanedithiol, 1,3-propanedithiol, 1,4-butanedithiol, 1,5-pentanedithiol, and 1,6-hexanedithiol showed that the carrier mobility decreased exponentially with increasing ligand length [79]. The carrier mobility of both carrier types increased by a factor of around 2.6 with every Angstrom decrease in ligand length [79]. The carriers' mobilities reached a maximum of 0.07 $cm^2 V^{-1} s^{-1}$ and 0.03 $cm^2 V^{-1} s^{-1}$ for electron and hole, respectively, with the shortest molecule EDT [79]. In the same study, the authors also showed the dependence of the carrier mobility on the QD size. It was shown that the electron mobility reaches a maximum for 6 nm sized PbSe QDs while the hole mobility increased with size [79].

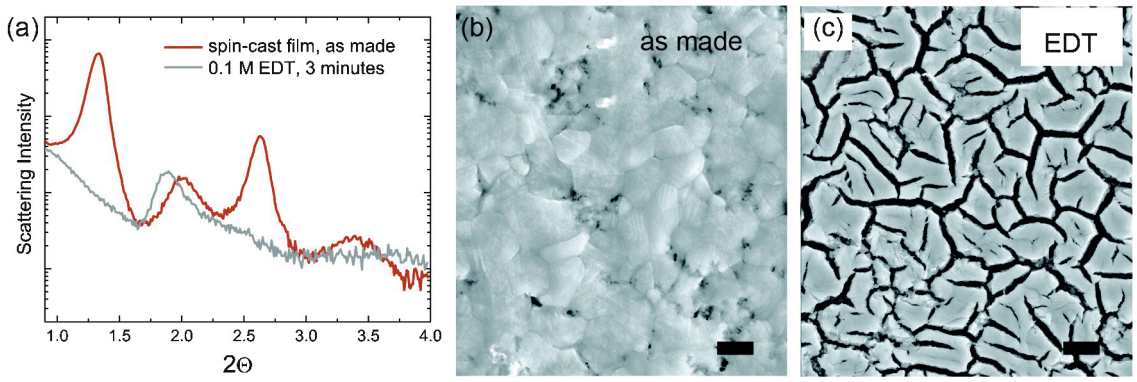

FIGURE 3

Microstructure of spin-cast PbSe QD films before and after EDT treatment (a) small-angle X-ray scattering data, showing ~16 Å decrease in QD spacing and dramatic loss of superlattice order upon EDT treatment. SEM images of (b) an untreated film and (c) a treated film. Untreated films have a peak-to-valley roughness of ±75 nm. Scale bar = 1 μm. Reprinted with permission from Ref. [55]. Copyright 2008 American Chemical Society.

Several other groups also studied the EDT treatment of PbS QDs in films [15,49,66,67,91,92]. Sargent *et al.* replaced the original oleic acid ligand with (very volatile) butylamine in solution and then treated the film with EDT [67]. The treatment resulted in a reduced interparticle spacing, which increased the hole mobility by a factor of 10 compared to untreated films to reach a value of 10^{-4} cm^2 V^{-1} s^{-1} [67]. At the same time, the EDT treatment reduced the doping level of the PbS QD solid. The reduced doping level was attributed to a reduction in the surface oxidation of QDs in the film which serves as a *p*-type dopant. The QD films could be re-doped again by heating in air without losing the gains in the carrier mobility [67].

A systematic study on the influence of EDT treated QD solids exposed to different gases was given by Norris *et al.*, which is very much needed for the application of EDT treated QD films in electronic or optoelectronic devices [93]. The group investigated the influence of N_2, O_2 and Ar for different exposure times and pressures on the electronic properties of PbSe solids. The fabrication and characterization of devices with QD solids will be done in most cases under inert atmosphere and the devices might be exposed to air somewhere during the process. Norris *et al.* found that ambient exposures longer than tens of seconds led to permanent and irreversible reductions in the carrier mobilities and a switch from ambipolar to *p*-type transport [93]. Surprisingly exposure to N_2 had an impact on the charge transport measurements in the PbSe films with electron mobility increasing, arguably because of passivation of electronic trapping sites by N_2. The increase in the electron mobility was reversible once N_2 was removed and the samples were put back into vacuum [93]. These results show that in the fabrication of QD sensitized optoelectronic devices special attention has to be given to the surrounding conditions.

Law *et al.* compared the effects of air exposure in PbS and PbSe QD films ligand exchanged with EDT and short-chain carboxylic acids [56]. The authors showed that films treated with carboxylic acids oxidized much slower upon air exposure than the films treated with EDT [56]. Hole mobilities reached up to 0.3 cm^2 V^{-1} s^{-1} for formic acid-treated PbSe QD films which makes the short-chain carboxylic acid treatment a viable option to increase efficiency and stability in QD solar cells [56]. In a similar vain, the same group also showed that atomic layer deposition (ALD) of Al_2O_3 or ZnO could prevent oxidation of PbSe QD films treated with short chain organic ligands, for example, EDT [80]. EDT treated PbSe QD films in-filled with Al_2O_3 and ZnO initially reached mobilities up to 1.05 cm^2 V^{-1} s^{-1} −1 (electron) and 0.04 cm^2 V^{-1} s^{-1} (hole) [80]. More recent work on ALD Al_2O_3 infilled QD FETs has pushed this still higher with electron mobilities exceeding 7 cm^2 V^{-1} s^{-1} [82].

Several groups also used ligand exchange with dithiocarbamates [57,94]. PbS QDs were ligand exchanged with strongly bonded *N*-2,4,6-trimethylphenyl-*N*-methyldithiocarbamate to protect them from oxidation in a solar cell [94]. Norris *et al.* performed ligand exchange on PbSe/CdSe core/shell and CdSe QDs with octyldithiocarbamate [57]. These ligands could be pyrolized at low enough temperatures to prevent the QDs from sintering and therefore kept the quantum confinement [57]. Other groups showed that QD ligands could be similarly removed by other means without compromising the quantum confinement, for example, by treatment with $(NH_4)_2S$ [95] or light exposure [96].

Amines

As well as the preceding body of early work on ligand exchange with thiols, several groups used different amines to increase the conductivity of QD films, especially hydrazine [7,47,78]. A treatment with hydrazine was demonstrated for a wide range of QDs: PbS [47,97], PbSe [32,47,78,98], PbTe [47,53], SnTe [52], CdSe [7,47] and InP [47]. Hydrazine treatment increases the conductivity of a QD solid via two mechanisms: first, depending on the chemical conditions, the long chain ligands used in the synthesis are replaced [32,98] and the interparticle spacing is reduced [47]; second, hydrazine acts as a *n*-type dopant, as previously observed for PbSe solids [32,47]. The carriers' mobilities reached a maximum of 0.9 cm^2 V^{-1} s^{-1} and 0.2 cm^2 V^{-1} s^{-1} for electrons and holes, respectively, for PbSe QD solids treated with hydrazine [47], and in a later study by Nozik *et al.*, reached 1.2 cm^2 V^{-1} s^{-1} for the electron mobility (in both cases a bottom-gate configuration was used) [78].

Several groups systematically extended the treatment of QD solids with other amines such as butylamine, methylamine, dodecylamine, octylamine, hexylamine, and pyridine [48,68,78]. For carbon QDs it was demonstrated that the mobilities decreased exponentially with the ligand length [68]. Yet,

even for the shortest amine used, pyridine, the mobilities reached not more than of 8.49×10^{-5} $cm^2 V^{-1} s^{-1}$ and 3.88×10^{-5} $cm^2 V^{-1} s^{-1}$ for electron and hole, respectively, in a bottom-gate configuration.

In more recent work, Talgorn *et al.* [64] have reported mobilities up to 3 $cm^2 V^{-1} s^{-1}$ for PbSe QD films with 1,2-ethanediamine as the ligand. Gao *et al.* [65] have also reported that diamines gave better mobilities in their PbSe QD FETs showing that the mobility scaled exponentially with ligand length. They also investigated bifunctional ligands with other head groups such as dithiols and dicarboxilic acids.

Even though the ligand exchange with short chain organic molecules improves charge carrier mobilities as reviewed above, it also has several disadvantages. Some of the chemicals used, for example hydrazine, are highly toxic [32]. As shown in Fig. 3, these treatments of QD films tend to lead to macroscopic cracks due to (ligand) volume losses [55]. A ligand exchange with organic molecules often changes QD properties through an increase of surface dangling bonds and mid-gap charge-trapping states [99]. Volume loss during the treatment is especially undesirable for optoelectronic devices since the macroscopic cracks could short circuit the device upon deposition of a top metal electrode [78]. To avoid short circuits, ligand exchange can alternatively be done in solution or it is also possible to do several cycles of a layer-by-layer deposition of QDs and a chemical (exchange) treatment on each cycle [55,78]. In 2010 Sargent *et al.* showed a solar cell with 5% efficiency in which a thick film was built up from several cycles of PbS QD deposition and chemical treatment with 3-mercaptopropionic acid (MPA) at each stage [100].

Inorganic: MCCs, metal-free ligands and ammonium thiocyanate

To avoid the disadvantages of ligand exchange with short chain organic molecules cited above, several research groups, foremost Talapin *et al.*, started to work on inorganic post-synthesis ligand treatments. In 2009 Talapin *et al.* proposed an all-inorganic ligand exchange with molecular metal chalcogenide complexes (MCCs) [69]. The use of different MCCs, such as SnS_4^{4-}, $Sn_2S_6^{4-}$, $SnTe_4^{4-}$, AsS_3^{3-}, MoS_4^{2-}, was shown for a number of QDs, such as CdSe, CdS, CdTe, PbS, PbTe, HgTe [58,69,99,101,102]. Besides strong chemical bonding, versatility and stability, using MCCs proved to be advantageous for charge transport in QD solids. The MCCs are smaller compared to organic ligands and have favourable HOMO and LUMO levels for charge transport, so that the ligand shell becomes less insulating [99]. Furthermore, upon heat treatment the MCCs transform into amorphous or crystalline metal chalcogenides with a weight loss as little as 3.8% so that crack-free QD solids with long-range order can be maintained [58,69]. In early experiments charge carrier mobilities of 0.03 $cm^2 V^{-1} s^{-1}$ in CdSe QD solids were achieved, demonstrating the potential of MCCs for efficient charge transport [69]. Further studies optimized the combination of QDs and MCC and the sample preparation method [59]. For a CdSe solid with $In_2Se_4^{2-}$ ligands band-like transport with a charge carrier mobility of up to 16 $cm^2 V^{-1} s^{-1}$ in the linear regime was demonstrated (Fig. 4) [59]. With a rapid thermal annealing treatment after deposition of the QDs, the same group just one year later showed a remarkable charge carrier mobility of up to 38 $cm^2 V^{-1} s^{-1}$ in a bottom-gate configuration [35].

Since foreign metal ions close to the QDs surface could potentially change the QD chemical and physical properties [103], Talapin *et al.* continued the work on inorganic ligand exchanges with metal-free inorganic ligands, such as S^{2-}, HS^-, Se^{2-}, HSe^-, Te^{2-}, HTe^-, TeS_3^{2-}, OH^-, NH_2^- [103]. For CdSe QDs with S^{2-} capping the mobilities reached 1.9 $cm^2 V^{-1} s^{-1}$ after annealing [35].

Claiming a more environmentally friendly approach, Kagan *et al.* used ammonium thiocyanate (NH_4SCN) for an inorganic ligand exchange, both in solution and film [73]. CdSe QDs ligand-exchanged in solution formed an *n*-type channel with mobilities up to 3 $cm^2 V^{-1} s^{-1}$ [73]. Several groups also used NaOH for ligand exchange in CdSe QD films [72,104]. In a top gate configuration with ion gels as a dielectric, mobilities up to 0.6 $cm^2 V^{-1} s^{-1}$ were observed [72]. Another inorganic ligand exchange strategy was demonstrated by Sargent *et al.* [66]. Figure 5 shows a scheme for atomic ligand passivation of PbS QDs with different halide anions (Cl^-, Br^- and I^-) [66]. This scheme increased the efficiency of QD sensitized solar cells to an impressive value of 6% in 2011 [66] and then crossed the 7% level in 2012 by a hybrid scheme of atomic ligand passivation in solution and organic ligand exchange in film [4]. Increased carrier mobilities (up to 4×10^{-2} $cm^2 V^{-1} s^{-1}$) were attributed to surface passivation and substitutional doping from the atomic ligand passivation with halide anions [77].

Recently, our group showed the synthesis of CdSe QDs with mercapto-substituted polyhedral oligomeric silsesquioxane (SH-POSS) as a surface ligand [105]. Even though POSS proved not to be a ligand favourable for charge transport in QD films [105], this example demonstrate that synthesis with ligands of specific functionalities other than the standard organic long chain alkyl molecules is possible.

As described above, different treatments of QDs have recently led to charge carrier mobilities higher than 30 $cm^2 V^{-1} s^{-1}$ which are approaching or even exceeding the values for organic-based FETs, for example, in polythiophene (typically below 0.05–0.1 $cm^2 V^{-1} s^{-1}$) [106], pentacene (typically up to 6 $cm^2 V^{-1} s^{-1}$) [106] or rubrene (more than 10 $cm^2 V^{-1} s^{-1}$) [107]. This impressive improvement in mobilities triggered the next step in research on QD based FETs [35]. To use QDs as active channels in commercial FETs, besides the charge carrier mobilities other parameters have to be optimized simultaneously. Commercial grade quantum dot FETs would require low operation voltages, small energy losses due to switching hysteresis and fast switching times [35]. For QD FETs there is still a lack of understanding of the charge transport mechanisms and nature of trapping sites and kinetics in different device geometries and material combinations and the influence of these issues on the mentioned parameters [35]. Consequently, QD based FETs showed much higher operational voltages than organic [108] or Si FETs [109] and strong hysteresis [35]. Switching times also remained largely uninvestigated in QD FETs before 2012 [35].

With the demonstration of high carrier mobilities, in 2012 Talapin *et al.* began to systematically investigate charge transport and trapping in different device geometries and material combinations to achieve simultaneously high carrier mobilities, low operational voltages, minimal hysteresis and fast switching speed [35]. For low operational voltage FETs there must be a strong capacitive coupling between the QD channel and the gate [35]. Also, the contact between the QD channel and the source and drain has to be optimized to minimize voltage drops at the

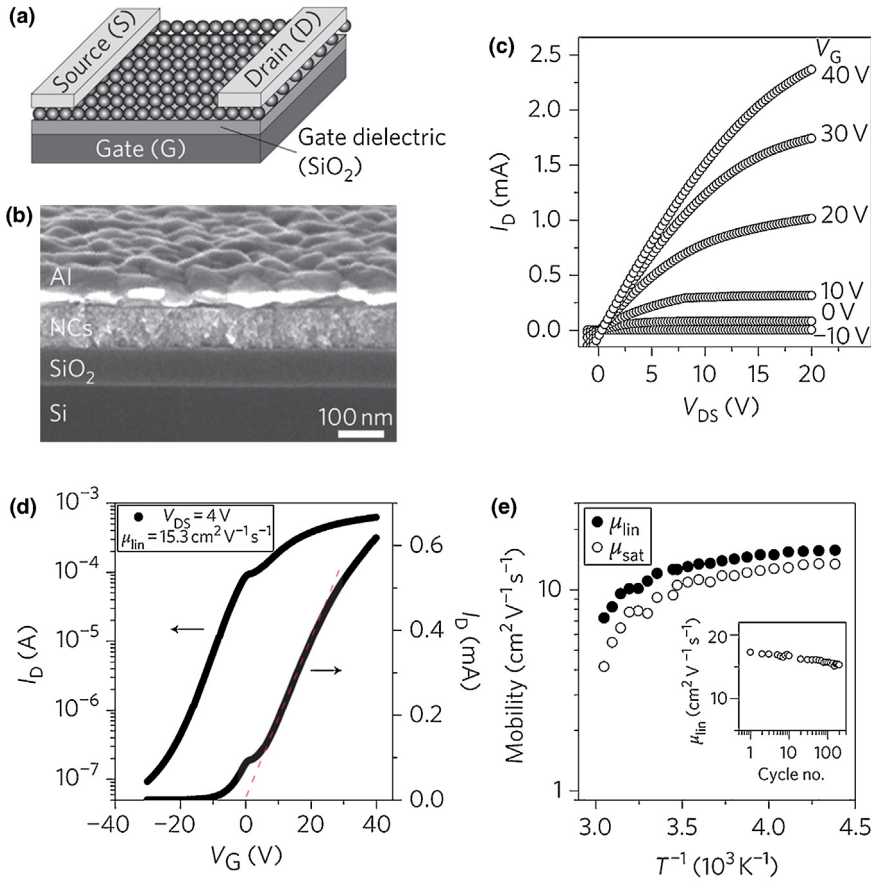

FIGURE 4

(a) QD FET schematic. (b) SEM of FET cross-section. (c) I_D vs. V_{DS} as a function of V_G for a device based on $In_2Se_4^{2-}$-capped 3.9 nm CdSe QDs (L = 50 μm, W = 450 μm). (d) I_D vs. V_G at V_{DS} = 4 V showing linear-regime field-effect mobility for an n-channel FET assembled from 3.9 nm CdSe QDs. (e) Temperature dependence of field-effect mobility for same device. (Inset) Evolution of field-effect mobility over 200 consecutive cycles of the gate voltage between −30 V and +30 V at V_{DS} = 2 V. The QD layer was annealed at 200 °C for 30 min (L = 72 mm, W = 954 μm). The thickness of the SiO_2 gate dielectric was 100 nm. Reprinted by permission from Macmillan Publishers Ltd: J.-S. Lee et al. [59], copyright 2011.

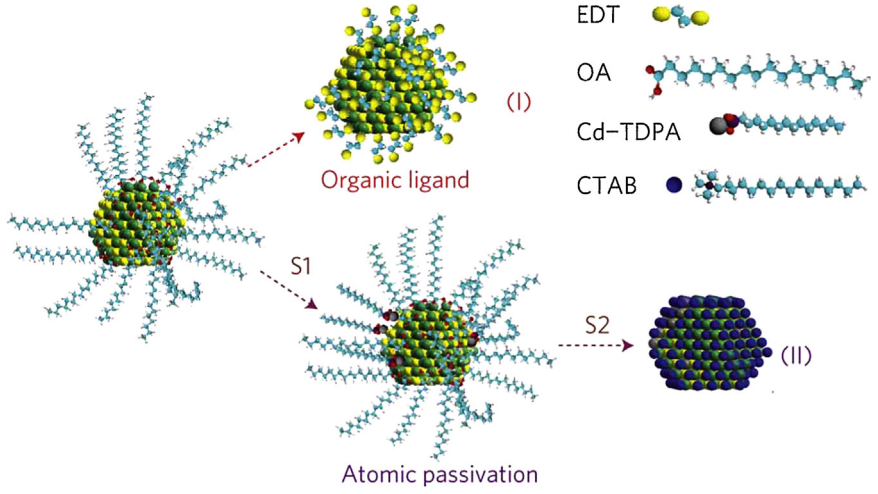

FIGURE 5

Organic and atomic ligand passivation strategies. PbS QDs having a Pb^{2+}-rich surface are initially capped with deprotonated oleic acid (OA). In the organic route, EDT substitutes the long OA ligands and binds to Pb^{2+} on the surface. In the atomic ligand route, a cadmium–tetradecylphosphonic acid (Cd–TDPA) complex was first introduced to the QD surface to passivate the exposed S^{2-} anions (S1). A solid-state halide treatment, for example, using cetyltrimethylammonium bromide (CTAB), introduced Br^- to cap the surface cations (S2). Colours are green (lead), yellow (sulphur), cyan (carbon), white (hydrogen), red (oxygen), grey (cadmium), blue (bromine) and purple (nitrogen). Adapted by permission from Macmillan Publishers Ltd: J. Tang et al. [66], copyright 2011.

electrodes [35]. In a bottom-gate configuration, thin ZrO_x film (6 nm) with a high dielectric constant ($\varepsilon \sim 9$) was used as the dielectric layer while the source and drain electrodes were Al. In this configuration a low operational voltage FET was demonstrated [35]. At the same time, these devices showed a strong hysteresis attributed to traps in the semiconducting channel [35,110] and at the semiconductor-dielectric interface due to hydroxyl groups at the ZrO_x surface [35,111]. To reduce the number of traps and consequently reduce hysteresis, in organic FETs an insulating ($\varepsilon \sim 2$) and hydroxyl-free fluoropolymer, Cytop, is widely used [35,112–114]. Talapin *et al.* showed that for QD FETs also the hysteresis could be minimized with Cytop as the dielectric layer in a top-gate configuration [35]. In addition these devices showed higher switching frequencies [35]. For the Cytop top-gate devices the mobilities remained lower than for the bottom-gate devices, which was attributed to a different dielectric capacitance and applied gate bias and a rough interface between QDs and the dielectric Cytop layer [35]. Alumina has been reported in a number of cases to be a good low hysteresis gate dielectric [26]. Kim *et al.* [36] have investigated the source of the hysteresis in SiO_2 dielectrics in studies on PbSe nanowire FETs and attributed it to the presence of surface water formed at the terminating silanol groups. Switching to Al_2O_3 reduced the hysteresis and further coating with PMMA helped as a water barrier (even low moisture levels in the glove box in which devices were processed had a noticeable effect on their devices). Silicon nitride, polyimide and parylene were also investigated, though all still showed a level of hysteresis. The most successful combination proved to be an alumina dielectric topped by a self-assembled monolayer (SAM) of octadecylphosphonic acid (ODPA), presumably largely due to the hydrophobicity of the alkylchain layer, borrowing from an approach similar to that used in organic FETs by Klauk *et al.* [33] Choi *et al.* [71] also investigated a hybrid Al_2O_3 topped SiO_2 dielectric.

This systematic approach to work on QD, gate and contact materials to simultaneously improve different FET parameters could pave the way to make the step for QD FETs from research to commercial products.

Chemical doping

Adding extra carriers into the film by chemical doping is another way to increase the conductivity of QD films [29]. The mobility of a QD based FET is a function of the Fermi level and chemical doping changes the Fermi-level range that is accessible. Chemical doping also opens the pathway for electronic and optical devices, for example, p–n junctions, that are conceptually similar to those that have been used in bulk semiconductor technology for decades [115–118]. In principle, two ways of doping have been explored in QDs: remote doping, where an electron donor is placed close to the QD surface and impurity doping [29]. However, controlling the process of doping has been proven very challenging for QDs [119]. Incorporating impurities into QDs, has been a synthetic challenge [38,119]. In most cases a doping precursor is included in the synthesis [70]. One difference relative to bulk semiconductors is the quantum confinement which leads to new phenomena in the doping process [70]. One of the models suggested to explain doping and its specific challenges in QDs is ''self-purification'' which means that the solubility of the impurity is much reduced in the QD compared to the bulk material [120,121]. The successful incorporation and foremost the location of the impurities in the QD can be also difficult to prove [70,119]. A further problem associated with the doping of QDs is that of determining the influence of the impurities on the structural, optical and electronic properties of the material. The Fermi level in a QD film depends on the number of electrons in the film. As described in the introduction, the turn-on voltage represents the difference between the Fermi level and the conduction band [38]. Therefore, FETs with impurity doped QD films are not only useful for measuring mobilities but also for determining the Fermi level which in return can give information about the impurities in the doped film [119]. Despite the challenges of doping QDs, on which several excellent papers and reviews were recently published [116,122–125], ''*doping the undopable*'' [126] has been shown to improve the conductivity in a number of QD based FETs:

- Remote doping of CdSe with sodium biphenyl [127]; of PbTe in a superlattice with Ag_2Te [54].
- Impurity doping of CdSe with Ag ions via a cation exchange [29] and with In and Al via a three-part core–shell synthesis [38]; of InAs doped with Cd [115] and with Cu, Ag or Au post-synthesis [128]; of PbSe with Ag via a partial cation exchange reaction [119]; of PbS and PbSe with excess Pb or Se by thermal evaporation into a QD film [81].

Kagan *et al.* and Talapin *et al.* extended the work on ligand exchanged QDs with MCCs, metal-free ligands and ammonium thiocyanate by doping these QDs with In and different cations [37,71]. Kagan *et al.* did a ligand exchange with ammonium thiocyanate in CdSe QDs and then doped QD films by thermal diffusion of indium [71]. The authors showed that the ligand exchange strongly coupled QDs which gave rise to band-like extended states in the film [71]. Doping with indium shifted the Fermi level above the trap levels so that these bands were accessible for transport [71]. Consequently, the mobilities increased to 27 $cm^2 V^{-1} s^{-1}$ [71].

Norris *et al.* demonstrated impurity doping of CdSe QDs with Al, In [38] and Ag [29]. Figure 6 shows FETs measurements on CdSe QD films doped with different amounts of Ag [29]. From the non-monotonic shifts in the turn-on voltage (Fig. 6b and d) and a comparison with silver doping of bulk semiconductors, the authors speculated that the doping changed from interstitial n-type to substitutional *p*-type with increased number of impurities [29]. The change in the Fermi level changed mobilities in the range from 0.01 to 0.1 $cm^2 V^{-1} s^{-1}$ depending on the doping level (Fig. 6e) [29]. Despite the clear influence of the Ag doping, the authors concluded that further work is necessary to gain a better fundamental understanding of doping in semiconductor QDs so it can be used in applications [29].

In very recent work, Murray and Kagan's groups showed that the carrier type, concentration, and Fermi level in QD films can be precisely controlled through the net dot stoichiometry [81]. The stoichiometry of colloidal QDs can be described by Hens' model of a stoichiometric ''bulk-like'' core with an outer shell of ions with a non-stoichiometric composition [118,129]. It has also been modelled that the effect on charge carrier transport by changing the stoichiometry might be especially pronounced in PbX (X = S or Se) QD films [116,118]. In the work of Murray and Kagan's groups the stoichiometry of ligand exchanged lead chalcogenide QD FETs was changed by introducing excess Pb or Se through thermal

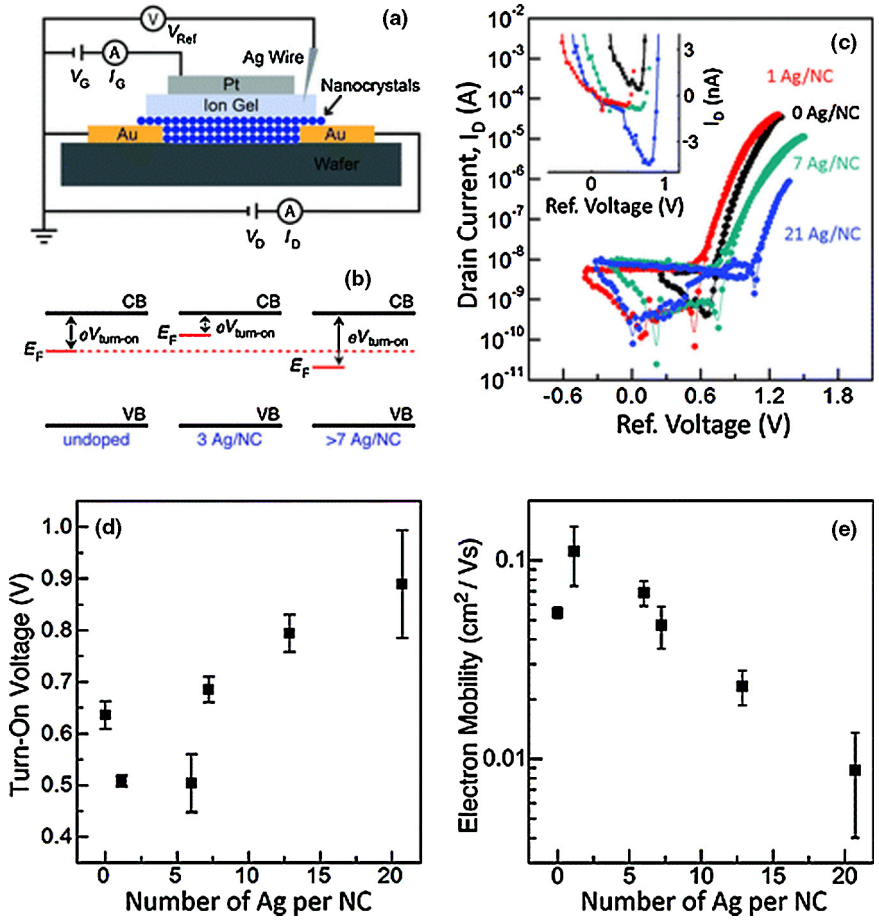

FIGURE 6

(a) Schematic cross section (not to scale) of ion-gel-gated thin-film transistors (*L* and *W*, 10 μm and 1 mm, respectively. (b) Energy-level diagram showing the Fermi energy, turn-on voltage, and the conduction band for films of CdSe nanocrystals (undoped, ~3 Ag/NC, and >7 Ag/NC). (c) I_D, versus the reference voltage, V_{ref}, for 3.6-nm-diameter nanocrystals with no Ag (black), 1.0 Ag/NC (0.13% Ag, red), 7.0 Ag/NC (0.85% Ag, green), and 21 Ag/NC (2.4% Ag, blue). V_D was 0.1 V, and V_{ref} was measured from an oxidized silver wire in the ion gel. The inset shows a magnified plot of the drain current near the turn-on voltage.

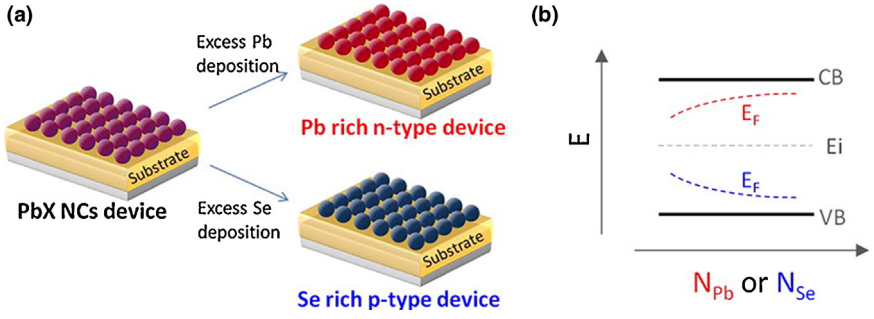

FIGURE 7

(a) Schematic of stoichiometric control of PbX nanocrystal (NC) thin films by Pb or Se deposition. (b) Fermi energy of PbX NCs as a function of the concentration of Pb (red) or Se (blue) atoms added to NC thin films. Reprinted with permission from Ref. [81]. Copyright 2013 American Chemical Society.

evaporation after deposition of the PbSe QD film [118]. The evaporation resulted in a shift of the Fermi level closer to the conduction band with Pb and closer to the valence band with Se (see Fig. 7) measured by changes in the threshold voltage [118]. Consequently, PbSe FETs showed *n*-type behaviour upon evaporation of Pb with linear electron mobilities of up to $9.0 \pm 2\ cm^2\ V^{-1}\ s^{-1}$ and *p*-type behaviour upon evaporation of Se with linear hole mobilities of $0.3 \pm 0.05\ cm^2\ V^{-1}\ s^{-1}$. Even though, doping of QDs by changing the stoichiometry in this study was successfully applied to increase the mobilities of FETs, it was still argued that its effect on surface trap states needs further exploration [118].

Prospects for quantum dot based FETs

Today's microelectronic devices are based on crystalline inorganic semiconductors like silicon with intrinsic mobilities (due to band-like transport rather than carrier hopping) that can reach $1000\ cm^2\ V^{-1}\ s^{-1}$ and device lifetimes over 50 years [1]. Despite

all the efforts in other material technologies this has been an unassailable truth for at least the last 50 years. With a size tunable band gap, a small exciton binding energy and high PL quantum yields, inexpensive solution processed colloidal semiconductor QDs offer great potential for use in electronic and optoelectronic devices [3,130]. Processing these QDs into devices is cheaper and, disentangled from the requirements of epitaxial growth on crystalline substrates, the materials are more versatile than other (bulk) crystalline inorganic semiconductors since low cost processes like spin coating and flexible plastic substrates can be used [3]. Despite these advantages, up to recently QD based FETs were rather used as a research tool, backing up promising results in carrier mobility and other studies in support of devices other than FETs, for example, QD based solar cells, rather than as electronic devices in their own right. That is because the traditional surface capping ligands, which are so necessary to regulate QD size and polydispersity during the growth, to prevent aggregation in solution and in summary to help achieve quantum confinement, form an insulating layer around the QDs that hinders efficient charge transport in a QD solid. There is an inherent contradiction between strong quantum confinement and electronic charge carrier transport [57]. However the body of work presented in this Review including examples of different treatments to improve charge carrier transport, shows that by applying judicious compromises vis-à-vis the ligands in the final processed films, QD based FETs are now reaching carrier mobilities comparable with organic FETs. In fact, as QD FET carrier mobilities have risen and the overall quality of the QD films has improved, several groups have started to report conduction mechanisms [64,71,76,82] which have attributes similar to band-like conduction in conventional bulk semiconductors such as silicon, and indeed this would be a very worthwhile objective to pursue. However, Guyot-Sionnest cautions in a recent Perspective article [131] that the negative temperature coefficient of mobility experimentally observed below some critical temperature value, is probably not a marker of the onset of band like hopping, but may still be consistent with a carrier hopping model. He argues that the size polydispersity, for example, gives rise to a disorder with an energy scale exceeding the coupling energy between dots and would therefore frustrate band-like conduction. Liu *et al.* [76] postulated that limited disorder might allow the formation of finite domains of a few dots extent wherein minibands may form, but still hopping dominates inter-domain communication of charge.

Notwithstanding the scope for eventually achieving band-like transport, the current debate is nonetheless a healthy sign of improving carrier mobilities. By crossing the mobility limit of 30 $cm^2 V^{-1} s^{-1}$ in 2012, scientists can now start to work on other parameters, like reducing hysteresis, lowering threshold voltages and the bias stress effect [92] to realize the full potential of solution processed colloidal QDs FETs. The way to achieve these goals could be guided by the results of research on organic FETs, as we have described it, for example, for the gate material. In addition, controlling the doping process will be an important aspect in the research on QD FETs and in the development of low-cost p–n junctions and bipolar transistors.

In terms of how close QD FET technology is to commercialization, Table 3 shows that though going head to head with conventional silicon CMOS on its home ground is a long way off and may never be realizable in terms of high mobility (high current) devices, there are performance areas where the processability and absence of the need for an epitaxial substrate, coupled with the potential for low cost fabrication should be starting to stimulate

TABLE 3

Comparison of some silicon CMOS and QD FET performance metrics.

Parameter	Silicon CMOS	QD FET	QD Ref.
Switching frequency	100s MHz–GHz	kHz–MHz	kHz [26], 10 kHz [132], MHz projected on basis of photo-conductivity in HgTe FET structures [133].
Hysteresis (ΔV_t)	No	0.25 V	CdSe [26]
Gate leakage current	Typically <pA/nm^2 with down to 1.5 nm gate oxide [134]	pA	CdSe [26] (gate dielectric limited so probably same for all – driven by geometry reduction)
Flexible/printable	No	Yes	[26]
Complimentary	Yes	Yes	PbSe (electron 9.6, hole 0.6 $cm^2 V^{-1} s^{-1}$ mobilities) [82]
Shelf life	50 years	10s days	In inert atmosphere
Operating life	50 years	10s days	In inert atmosphere
O_2 sensitivity	No	Yes	Need barrier layers
Scale	90 nm (CMOS ASICs) (Intel are reaching 22 nm)	Typically (10 × 100) μm	CdSe [26]
Max process temperature	High	Low	
Electron mobility	1400 $cm^2 V^{-1} s^{-1}$ [135]	38 $cm^2 V^{-1} s^{-1}$	CdSe [35]
Hole mobility	450 $cm^2 V^{-1} s^{-1}$ [135]	2.38 $cm^2 V^{-1} s^{-1}$	HgTe [74]
Band-like transport	Yes	Not to date	See [131]
On-off current ratio	Commercial	10^6	CdSe [26]
Threshold voltage	Typ 0.2 V	0.38 V	CdSe [26]
Predominant QD types		PbSe, PbS, CdSe, InAs, InSb, InP, HgTe	
Carrier densities			
Electrons	Similar to usual *n*-type Si ranges	$10^{19}/cm^3$	PbSe/Pb [81]
Holes	Similar to usual *p*-type Si ranges	$10^{18}/cm^3$	PbSe/Se [81]

interest in commercial development. The demonstration of flexible QD FET circuitry by Kim *et al.* [26] is an outstanding example of how QD FETs may gain a foothold by initially developing as a niche technology (low cost, low power, flexible devices). In addition, Guyot-Sionnest [131] makes the point that QD films used in FETs may already have surpassed the mobilities (e.g. $>0.1\ cm^2\ V^{-1}\ s^{-1}$) for low current applications such as photodetectors, or photovoltaic cells.

Further work to develop QD FETs will doubtlessly go hand in hand with continuing efforts to develop colloidal QD films for other devices like solar cells and sensors. For example, Koppens *et al.* [136] recently showed how to achieve high sensitivity in a photodetector by combining the optical properties of QDs with the transport properties of graphene. Due to the outlined potential of colloidal QDs for electronic and optoelectronic applications and the impressive improvements in the last few years we expect that colloidal QD FETs will continue to make the step from research driven by scientific curiosity to economically attractive commercial applications in the near future.

Acknowledgements

We gratefully acknowledge funding from the Research Grants Council of the Hong Kong S.A.R., China (projects 102412, 102810, 4055012), an Applied Research Grant of City University of Hong Kong (9667067), and the National Science Foundation of China (Grant no. A.03.13.01401).

References

[1] B.A. Ridley, et al. Science 286 (1999) 746–749.
[2] A.I. Ekimov, A.A. Onushchenko, Soviet J. Exp. Theor. Phys. Lett. 34 (1981) 345.
[3] D.V. Talapin, et al. Chem. Rev. 110 (2010) 389–458.
[4] A.H. Ip, et al. Nat. Nanotechnol. 7 (2012) 577–582.
[5] S.V. Kershaw, et al. Chem. Soc. Rev. 42 (2013) 3033–3087.
[6] J.E. Murphy, et al. J. Phys. Chem. B 110 (2006) 25455–25461.
[7] D. Yu, et al. Science 300 (2003) 1277–1280.
[8] P. Liljeroth, et al. Phys. Rev. Lett. 97 (2006) 096803.
[9] W.-k. Koh, et al. Nano Lett. 11 (2011) 4764–4767.
[10] C.B. Murray, et al. Annu. Rev. Mater. Sci. 30 (2000) 545–610.
[11] A.J. Houtepen, et al. J. Am. Chem. Soc. 128 (2006) 6792–6793.
[12] M.A. Hines, G.D. Scholes, Adv. Mater. 15 (2003) 1844–1849.
[13] S.A. McDonald, et al. Appl. Phys. Lett. 85 (2004) 2089–2091.
[14] G. Konstantatos, et al. Adv. Funct. Mater. 15 (2005) 1865–1869.
[15] K.S. Jeong, et al. ACS Nano 6 (2011) 89–99.
[16] H. Liu, et al. J. Am. Chem. Soc. 129 (2006) 305–312.
[17] A.A. Guzelian, et al. Appl. Phys. Lett. 69 (1996) 1432–1434.
[18] W. Liu, et al. J. Am. Chem. Soc. 134 (2012) 20258–20261.
[19] M.V. Kovalenko, et al. J. Am. Chem. Soc. 128 (2006) 3516–3517.
[20] A.L. Rogach, et al. Berichte der Bunsengesellschaft für physikalische Chemie 100 (1996) 1772–1778.
[21] N. Gaponik, et al. Nano Lett. 2 (2002) 803–806.
[22] H. Sun, et al. Chem. Mater. 20 (2008) 6764–6769.
[23] E.V. Shevchenko, et al. J. Am. Chem. Soc. 127 (2005) 8741–8747.
[24] S.M. Rupich, et al. J. Am. Chem. Soc. 132 (2009) 289–296.
[25] B. Lee, et al. J. Am. Chem. Soc. 131 (2009) 16386–16388.
[26] D.K. Kim, et al. Nat. Commun. 3 (2012) 1216.
[27] G. Horowitz, Adv. Mater. 10 (1998) 365–377.
[28] J. Robertson, Eur. Phys. J. Appl. Phys. 28 (2004) 265–291.
[29] A. Sahu, et al. Nano Lett. 12 (2012) 2587–2594.
[30] J.H. Cho, et al. Nat. Mater. 7 (2008) 900–906.
[31] P. Fontaine, et al. Appl. Phys. Lett. 62 (1993) 2256–2258.
[32] M.S. Kang, et al. Nano Lett. 9 (2009) 3848–3852.
[33] H. Klauk, et al. Nature 445 (2007) 745–748.
[34] I. Mejia, M. Estrada, in: Proceedings of the 6th International Caribbean Conference, 2006, pp. 375–377.
[35] D.S. Chung, et al. Nano Lett. 12 (2012) 1813–1820.
[36] D.K. Kim, et al. ACS Nano 5 (2011) 10074–10083.
[37] A. Nag, et al. J. Am. Chem. Soc. 134 (2012) 13604–13615.
[38] A.W. Wills, et al. J. Mater. Chem. 22 (2012) 6335–6342.
[39] A.L. Roest, et al. Phys. Rev. Lett. 89 (2002) 036801.
[40] A.L. Roest, et al. Appl. Phys. Lett. 83 (2003) 5530–5532.
[41] A.L. Roest, et al. Faraday Discuss. 125 (2004) 55–62.
[42] A.J. Houtepen, D. Vanmaekelbergh, J. Phys. Chem. B 109 (2005) 19634–19642.
[43] R.E. Chandler, et al. Phys. Rev. B 75 (2007) 085325.
[44] A.J. Houtepen, et al. Nano Lett. 8 (2008) 3516–3520.
[45] B.L. Wehrenberg, et al. J. Phys. Chem. B 109 (2005) 20192–20199.
[46] D. Yu, et al. Phys. Rev. Lett. 92 (2004) 216802.
[47] D.V. Talapin, C.B. Murray, Science 310 (2005) 86–89.
[48] S. Geyer, et al. Phys. Rev. B 82 (2010) 155201.
[49] J. Tang, et al. ACS Nano 4 (2010) 869–878.
[50] T. Hanrath, J. Vac. Sci. Technol. A: Vac. Surf. Films 30 (2012) 030802.
[51] H. Kim, et al. Electron Device Lett., IEEE 28 (2007) 42–44.
[52] M.V. Kovalenko, et al. J. Am. Chem. Soc. 129 (2007) 11354–11355.
[53] J.J. Urban, et al. J. Am. Chem. Soc. 128 (2006) 3248–3255.
[54] J.J. Urban, et al. Nat. Mater. 6 (2007) 115–121.
[55] J.M. Luther, et al. ACS Nano 2 (2008) 271–280.
[56] M.H. Zarghami, et al. ACS Nano 4 (2010) 2475–2485.
[57] A.W. Wills, et al. ACS Nano 4 (2010) 4523–4530.
[58] M.V. Kovalenko, et al. J. Am. Chem. Soc. 132 (2010) 15124–15126.
[59] J.-S. Lee, et al. Nat. Nanotechnol. 6 (2011) 348–352.
[60] P. Guyot-Sionnest, C. Wang, J. Phys. Chem. B 107 (2003) 7355–7359.
[61] C.A. Leatherdale, et al. Phys. Rev. B 62 (2000) 2669–2680.
[62] M.V. Jarosz, et al. Phys. Rev. B 70 (2004) 195327.
[63] E. Talgorn, et al. J. Phys. Chem. C 114 (2010) 3441–3447.
[64] E. Talgorn, et al. Nat. Nano 6 (2011) 733–739.
[65] Y. Gao, et al. ACS Nano 6 (2012) 9606–9614.
[66] J. Tang, et al. Nat. Mater. 10 (2011) 765–771.
[67] E.J.D. Klem, et al. Appl. Phys. Lett. 92 (2008) 212105.
[68] W. Kwon, et al. ACS Appl. Mater. Interface 5 (2013) 822–827.
[69] M.V. Kovalenko, et al. Science 324 (2009) 1417–1420.
[70] D.J. Norris, et al. Science 319 (2008) 1776–1779.
[71] J.-H. Choi, et al. Nano Lett. 12 (2012) 2631–2638.
[72] M.S. Kang, et al. Nano Lett. 10 (2010) 3727–3732.
[73] A.T. Fafarman, et al. J. Am. Chem. Soc. 133 (2011) 15753–15761.
[74] H. Kim, et al. Appl. Phys. Lett. 89 (2006) 173107.
[75] M. Soreni-Harari, et al. Adv. Funct. Mater. 20 (2010) 1005–1010.
[76] W. Liu, et al. J. Am. Chem. Soc. 135 (2012) 1349–1357.
[77] D. Zhitomirsky, et al. Adv. Mater. 24 (2012) 6181–6185.
[78] M. Law, et al. J. Am. Chem. Soc. 130 (2008) 5974–5985.
[79] Y. Liu, et al. Nano Lett. 10 (2010) 1960–1969.
[80] Y. Liu, et al. Nano Lett. 11 (2011) 5349–5355.
[81] S.J. Oh, et al. ACS Nano 7 (2013) 2413–2421.
[82] Y. Liu, et al. Nano Lett. 13 (2013) 1578–1587.
[83] S.J. Oh, et al. ACS Nano 6 (2012) 4328–4334.
[84] H.E. Romero, M. Drndič, Phys. Rev. Lett. 95 (2005) 156801.
[85] M. Drndič, et al. J. Appl. Phys. 92 (2002) 7498–7503.
[86] Z. Hu, et al. Nano Lett. 5 (2005) 1463–1468.
[87] T.S. Mentzel, et al. Phys. Rev. B 77 (2008) 075316.
[88] G. Konstantatos, et al. Nature 442 (2006) 180–183.
[89] K.S. Leschkies, et al. ACS Nano 3 (2009) 3638–3648.
[90] M.S. Kang, et al. Nano Lett. 11 (2011) 3887–3892.
[91] P. Nagpal, V.I. Klimov, Nat. Commun. 2 (2011) 486.
[92] T.P. Osedach, et al. ACS Nano 6 (2012) 3121–3127.
[93] K.S. Leschkies, et al. J. Phys. Chem. C 114 (2010) 9988–9996.
[94] R. Debnath, et al. J. Am. Chem. Soc. 132 (2010) 5952–5953.
[95] H. Zhang, et al. Nano Lett. 11 (2011) 5356–5361.
[96] W.J. Kim, et al. Nano Lett. 8 (2008) 3262–3265.
[97] J.-S. Lee, et al. J. Am. Chem. Soc. 130 (2008) 9673–9675.
[98] K.J. Williams, et al. ACS Nano 3 (2009) 1532–1538.
[99] M.V. Kovalenko, et al. J. Am. Chem. Soc. 132 (2010) 10085–10092.
[100] A.G. Pattantyus-Abraham, et al. ACS Nano 4 (2010) 3374–3380.
[101] M.V. Kovalenko, et al. J. Am. Chem. Soc. 134 (2012) 2457–2460.
[102] E. Lhuillier, et al. Adv. Mater. 25 (2013) 137–141.
[103] A. Nag, et al. J. Am. Chem. Soc. 133 (2011) 10612–10620.
[104] D. Yu, et al. J. Appl. Phys. 99 (2006) 104315.
[105] Y. Wang, et al. J. Phys. Chem. C 117 (2013) 1857–1862.
[106] H. Klauk, Chem. Soc. Rev. 39 (2010) 2643–2666.
[107] D. Braga, G. Horowitz, Adv. Mater. 21 (2009) 1473–1486.

[108] M. Halik, et al. Nature 431 (2004) 963–966.
[109] J. Collet, D. Vuillaume, Appl. Phys. Lett. 73 (1998) 2681–2683.
[110] G. Gu, et al. Appl. Phys. Lett. 87 (2005) 243512.
[111] L.-L. Chua, et al. Nature 434 (2005) 194–199.
[112] J. Veres, et al. Chem. Mater. 16 (2004) 4543–4555.
[113] W.L. Kalb, et al. Appl. Phys. Lett. 90 (2007) 092104.
[114] T. Sakanoue, H. Sirringhaus, Nat. Mater. 9 (2010) 736–740.
[115] S.M. Geyer, et al. ACS Nano 4 (2010) 7373–7378.
[116] O. Voznyy, et al. ACS Nano 6 (2012) 8448–8455.
[117] J. Tang, et al. Nano Lett. 12 (2012) 4889–4894.
[118] J.M. Luther, J.M. Pietryga, ACS Nano 7 (2013) 1845–1849.
[119] M.S. Kang, et al. Adv. Mater. 25 (2013) 725–731.
[120] F.V. Mikulec, et al. J. Am. Chem. Soc. 122 (2000) 2532–2540.
[121] G.M. Dalpian, J.R. Chelikowsky, Phys. Rev. Lett. 96 (2006) 226802.
[122] D.H. Son, et al. Science 306 (2004) 1009–1012.
[123] S.C. Erwin, et al. Nature 436 (2005) 91–94.
[124] J.D. Bryan, D.R. Gamelin, Progress in Inorganic Chemistry, John Wiley & Sons, Inc., 2005, pp. 47–126.
[125] B. Skinner, et al. Phys. Rev. B 85 (2012) 205316.
[126] G. Galli, Nature 436 (2005) 32–33.
[127] M. Shim, P. Guyot-Sionnest, Nature 407 (2000) 981–983.
[128] D. Mocatta, et al. Science 332 (2011) 77–81.
[129] I. Moreels, et al. Chem. Mater. 19 (2007) 6101–6106.
[130] F. Hetsch, et al. J. Phys. Chem. Lett. 2 (2011) 1879–1887.
[131] P. Guyot-Sionnest, J. Phys. Chem. Lett. 3 (2012) 1169–1175.
[132] S.H. Im, et al. Energy Environ. Sci. 4 (2011) 4181–4186.
[133] M. Chen, et al. Adv. Funct. Mater. (2011), http://dx.doi.org/10.1002/adfm.201301006.
[134] S. Suthram, et al., Leakage in Nanometer CMOS Technologies, Series: Integrated Circuits and Systems, Springer, 2006p. 287 Chapter 12.
[135] See database at: http://www.ioffe.rssi.ru/SVA/NSM/Semicond/Si/electric.html.
[136] G. Konstantatos, et al. Nat. Nanotechnol. 7 (2012) 363–368.